Research Article
Open Access

Life Sciences, Medicine and Biomedicine

Alteration of pulmonary mitochondrial oxidation status, inflammation, energy metabolizing enzymes, oncogenic and apoptotic markers in mice model of diisononyl phthalate-induced asthma

Samuel Abiodun Kehinde[1], Abosede Temitope Olajide[2,*], Oyindamola Joy Akinpelu[3] and Sanmi Tunde Ogunsanya[4]

[1]Department of Environmental Health Science, Faculty of Basic Medical Sciences, Ajayi Crowther University, Oyo, Nigeria. Postcode: 211251.
[2]Cell and Signalling unit, Department of Biomedical Science, Faculty of Medicine and Health Sciences, Universiti Putra Malaysia, Malaysia. Postcode: 43400.
[3]Biochemistry unit, Department of Chemical Sciences, Faculty of Natural Sciences, Ajayi Crowther University, Oyo, Nigeria. Postcode: 211251.
[4]Anatomy Unit, Faculty of Basic Medical Sciences, Ajayi Crowther University, Oyo, Nigeria. Postcode: 211251.

***Correspondence:** at.olajide@acu.edu.ng

Received: 20 March 2023; **Revised:** 23 June 2023; **Accepted:** 14 August 2023; **Published:** 24 September 2023
DOI https://doi.org/10.28916/lsmb.7.1.2023.113

ABSTRACT

Primary plasticizer used in polyvinyl chloride is diisononyl phthalate (DiNP) and exposure to DiNP has been associated with the development of asthma and allergies. In the current study, how DiNP alters pulmonary antioxidant status, inflammation, energy metabolizing enzymes, oncogenic and apoptotic markers in DiNP-induced asthmatic mice was examined. Male BALB/c mice (n=20, 20-30 g) were divided into 2 groups of 10 mice each: group 1 (control) received saline (0.2ml/kg) orally for 23 days, and group 2 (DiNP) received 50 mg/kg DiNP (Intraperitoneal and intranasal) once per day. After the last administration, mice were sacrificed, lungs were removed and used for biochemical and histopathological analysis. DiNP treated mice experienced alterations in their lung histoarchitecture, levels of oncogenic and apoptotic factors, glycolytic, tricarboxylic acid cycle (TCA), and electron transport chain enzymes (ETC), antioxidant status, and inflammatory biomarkers. DiNP decreased the lungs levels of reduced glutathione and ascorbic acid, and the activities of superoxide dismutase, catalase, and glutathione-s-transferase. In the lungs of DiNP-treated mice compared to the control group, malondialdehyde and inflammatory biomarkers (nitric oxide and myeloperoxidase) were significantly greater ($p<0.05$). Furthermore, the activities of glycolytic enzymes hexokinase, aldolase, lactate dehydrogenase were downregulated with a concomitant increase in NADase (77%). TCA enzymes and ETC enzymes were significantly reduced as well. CAS-3, p53, Bax, c-MYC, K-Ras increased by 65%, 51%, 70%, 59% and 82% respectively while BCL-2 decreased by 74%. Histopathological analysis revealed distortion of the airway structure characterized by inflammatory cell infiltration, oedema, hemorrhage, and constricted alveoli space. Exposure to DiNP caused oxidative stress which promotes lung inflammation via depletion of antioxidants, pulmonary energy transduction enzymes, levels of oncogenic and apoptotic factors were impaired as well, suggesting that the lungs may not be able to perform its morphological and physiological functions effectively.

Keywords: *Diisononyl phthalates; asthma; mitochondrial metabolizing enzymes; oxidative stress and apoptotic markers*

INTRODUCTION

The symptoms of allergic asthma include airway inflammation, airway hyperresponsiveness (AHR), and elevated serum immunoglobulin E (IgE) levels. Allergic asthma is a chronic inflammatory condition of the airways. The frequency of asthma has been increasing worldwide over the previous few decades with a foresight of more increase of 325 million (Pawankar, 2014). Recent epidemiological studies have demonstrated a strong correlation between exposure to phthalate pollutants, such as diisononyl phthalate (DiNP; Figure 1), and the prevalence of allergic asthma. Phthalate esters are often colourless, clear, viscous liquids that resemble oils. Phthalates are mostly employed as plasticizers, which means that they are added to polymers to improve the materials' pliability and tensile strength. Toys, construction materials, auto parts, electronic and medical components, and many more plastic products use plasticizers extensively (Tang et al., 2015).

It has been demonstrated that exposure to DiNP causes allergic airway inflammation in rats via activating the PI3K/Akt pathway. More recent studies have shown that DiNP promotes Th2 polarisation from naive CD4+ T cells and suppresses Th1 differentiation from these cells in vitro. These studies also showed that animals exposed to and challenged with DiNP experienced Th2 type immune responses that involved the up-regulation of Th2-mediated cytokines or immunoglobulin E in vivo.(Chen et al., 2015). These studies demonstrate that DiNP poses a risk for human asthma induction (Chen et al., 2015; Hwang et al., 2017). Also, it has been acknowledged that the phthalate esters chemical family, which is widely used in the environment, poses a growing risk to human health, including cancer (Hsieh et al., 2012). In addition, a variety of substrates are used by the lung as vital synthesis building blocks, fuels for generating energy, sources of NADPH for lipid biosynthesis, and glutathione sources. These substrates consist of amino acids, glucose, lactate, fatty acids, choline, and ketone bodies (Liu & Summer, 2019). However, DiNP has been demonstrated in previous studies to interfere with energy metabolism of different organs in murine models by causing perturbations in the glycolytic, tricarboxylic acid cycle and electron transport chain enzymes (Kehinde et al., 2022a; Kehinde et al., 2022b; Kehinde et al., 2023). In the current study, how DiNP alters pulmonary antioxidant status, inflammation, energy metabolizing enzymes, oncogenic and apoptotic markers in DiNP-induced asthmatic mice was examined.

Figure 1

Chemical structure of Diisononyl phthalate (Bis(7-methyloctyl) benzene-1,2-dicarboxylate)

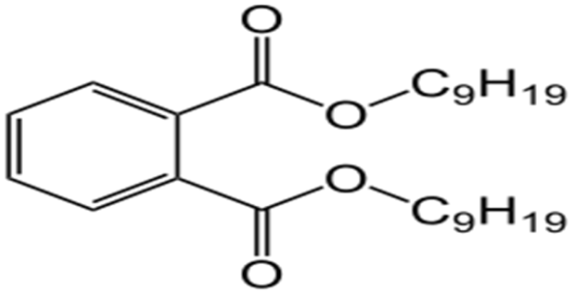

Note: (Chiu et al., 2020)

METHODOLOGY

Chemicals and reagents

Chemicals used for this study included diisononyl phthalate, mannitol, sucrose, sorbitol, glucose-6-phosphate dehydrogenase, ethylenediaminetetraacetic acid (EDTA), Nicotinamide adenine dinucleotide (NADH), fructose-1,6-bisphosphate, succinate, Bovine Serum Albumin, Phospohenolpyruvate, oxaloacetate, Rotenone, cytochrome c, and tris(hydroxymethyl)aminomethane (Trizma base). These were products of AK Scientific, USA. Diagnostic kits for the assays and determination of total protein determination and lactate dehydrogenase were products of CYPRESS® Diagnostics, Langdorp, Belgium. The investigation also used several reagents, all of which were of analytical quality.

Equipment

Equipment used in the course of this study were Beckman® Ultracentrifuge, model PN LL-IM-12AB (Beckman Coulter, Inc. 250 S, Kraemer Boulevard, Brea, California, USA), T90+ UV/VIS Spectrophotometer (PG instrument Limited, Beijing, China), JOL-802 Centrifuge, model HEM-412C (Jintan Medical Instrument Factory, Jiangsu, China), pH meter, Rex model pHs 25(Ningbo Biocotek Scientific Instrument Company Limited, China), and Mettler H10 analytical balance (Mettler-Toledo, Polaris Parkway, Columbus, Ohio, USA).

Experimental animals

For this study, twenty (20) healthy male BALB/c mice weighing 20–30 g were used. The animals were from the University of Ibadan's Veterinary Anatomy Department's animal holdings. They were raised at Ajayi Crowther University Oyo's Department of Biochemistry. Prior to the start of the study, the mice were given a week of acclimatization and were given unlimited access to standard laboratory food and water ad libitum. Mice were kept in a natural environment with a 12-hour cycle of light and darkness at a temperature of 22–25 °C. The Ethical Review Committee of the Faculty of Natural Sciences at Ajayi Crowther University approved the study's experimental design with ethical number FNS/ERC/23/005AP.

Induction of asthma

The intraperitoneal injection of 50 mg/kg of DiNP in 0.2 mL of saline on day 0 was the main method used to sensitize the mice. On days 3 and 10, intraperitoneal injections of 50 mg/kg of DiNP dissolved in saline were used to secondarily sensitize the mice. On days 19, 21, and 23, the mice were given an intranasal injection of 50 mg/kg of DiNP diluted in 50 mL of saline. The intranasal injection of 50mg/kg of DiNP was 50µL (Olajide et al., 2023).

Figure 2

DiNP-induced asthma experimental design

Preparation of lung homogenate

Each mouse's lungs were carefully removed, immediately rinsed in 1.15% potassium chloride (KCl), and then homogenized in 5 mL of 0.1 M phosphate buffer pH 7.4. For the biochemical and molecular tests, the post mitochondrial supernatant was obtained by centrifuging the homogenates at 10,000 x g for 15 min at 4°C.

Isolation of mitochondria from the lungs

Lungs were obtained from the mice and washed in 1.15% KCl. The organ was then homogenized using homogenization medium (5w/v: sucrose, 2M EDTA, 0.5M TRIS-HCl. pH 7.4) and centrifuged at 3000 rpm for 5 mins. The supernatant was removed into 5 mL Eppendorf tubes and centrifuged at 13000 rpm for 2 mins. The pellet which contains the mitochondria was washed with homogenization medium, transferred to an already weighed 2 mL Eppendorf tube and centrifuged at 13000 rpm for 2 mins. The supernatant was decanted and pellets resuspended in MAITE medium (sucrose, sorbitol, 0.5M EDTA, KCL, 1M MgCL2, 0.5M TRIS-KCl, Orthophosphoric acid. pH 7.4). It was centrifuged for 2 mins at 13000 rpm and the supernatant decanted. The 2 mL Eppendorf tube containing the mitochondria was re-weighed and the weight of empty Eppendorf tube was subtracted from the weight of Eppendorf tube containing isolated mitochondria. This gave the weight of mitochondria obtained. The mitochondria isolate was resuspended in 1 mL of MAITE medium and stored. All homogenization and centrifugation were carried out at 4^{o}C (Liao et al., 2020).

Assessment of pulmonary oxidative imbalance and redox state biomarkers in asthmatic mice

The lipid peroxidation marker, malondialdehyde concentration (MDA) was determined by the method of Buege and Aust (1978). In this method, 0.1 mL of the lung sample was mixed with 2 mL of the TCA/TBA/HCl (1:1:1) reagent before boiling at 100 °C for 15 minutes and letting the mixture cool. By centrifuging the materials for 10 minutes at 3000 rpm, flocculent elements were removed. After removing the supernatant, the absorbance was measured at 532 nm against a blank. The MDA concentration was determined using the 1.55 × 106 M− 1 cm− 1 molar extinction coefficient for the MDA-TBA combination.

The method of Moron et al. (1979) was used to measure the amount of lung reduced glutathione (GSH). Sulphosalicyclic acid was diluted 1:1 with the lung sample, and the mixture was centrifuged at 3000 rpm for five minutes. After adding 0.5 mL of the supernatant to a solution containing 4 mL of 0.1 M phosphate buffer (pH 7.4) and 0.5 mL of Ellman's reagent, the resultant colour was detected at 412 nm.

The Habig et al. (1974) approach was used to calculate the lung glutathione S-transferase (GST) activity using the enzyme-catalyzed condensation of glutathione with 1-chloro-2,4-dinitrobenzene. 30 µL of reduced glutathione, 150 µL of 2,4-dinitrochlorobenzenne (CDNB), 2.79 mL of 0.1 M phosphate buffer (pH 6.5), and 30 µL of lung sample make up the reaction mixture, to put it briefly. It was thoroughly mixed, and for three minutes, the absorbance was measured at 340 nm every minute.

The Misra and Fridovich (1972) approach was used to assess the lung activity of superoxide dismutase (SOD). The technique is based on SOD's capacity to prevent adrenaline's self-oxidation into adrenochrome at alkaline pH. The reaction mixture contains 0.3 mL of adrenaline, 2.5 mL of 0.05 M sodium bicarbonate buffer (pH 10.2), and 0.2 mL of the lung sample. The reaction mixture was mixed in the cuvette before being read at 480 nm. The enzyme necessary to 50% block adrenaline autooxidation is considered to be one unit of enzyme activity. The Sinha (1972) method was used to measure the lung catalase's (CAT) activity. Lung homogenate (0.25 mL), 0.01 M phosphate buffer (pH 7.0), and 2 M H2O2 were all included in the reaction mixture (1 mL). At 0, 1, 2, and 3 minutes, 0.5 mL of dichromate-acetic acid reagent—5% potassium dichromate and glacial acetic acid—was added to stop the reaction. After 10 minutes of heating in boiling water, the mixture was then cooled to room temperature. At 570 nm, the absorbance was measured. The method established by Jagota and Dani (1982) was used to measure the amount of ascorbic acid (AA) in lung homogenate. In the Folin-Ciocalteu method, AA in biological samples reacts with the reagent to produce a blue colour with a maximum absorbance at 760 nm.

Evaluation of pulmonary inflammation biomarker in asthmatic mice

The amount of nitric oxide (NO) in the lungs was calculated using the nitrite ion detection Griess Reagent (Green et al., 1982). 50 µL of sample, 150 µL of sulfanilamide, and 100 µL of distilled water made up the reaction mixture. Following the addition of 150 µL of N-naphthyl ethylenediamine, the mixture was incubated for an additional 10 min. The system's production of NO was represented by the concentration of the nitrite ion, which was measured at 540 nm. The method as described by Kim (2012) was used to measure the spectrophotometric activity of myeloperoxidase (MPO). 10 µL of the sample, 80 µL of 0.75 mM H_2O_2, and 110 µL of the TMB solution were put into a plate (2.9 mM TMB in 14.5 percent DMSO and 150 mM sodium phosphate buffer at pH 5.4). After that, the plate was incubated for 5 minutes at 37°C. The reaction was halted after adding 50 µL of 2M H_2SO_4, and the myeloperoxidase (MPO) activity was determined using the absorbance at 450 nm.. At mg/tissue, MPO activity was calculated.

Determination of pulmonary glycolytic enzymes activities in asthmatic mice

The method outlined by Colowick was followed to determine the activity of hexokinase (HK). By measuring the rise in absorbance at 340 nm, an assay based on the reduction of NAD+ through a coupled reaction with glucose-6-phosphate dehydrogenase (G-6-P-D) was developed (Colowick & Schmidt, 1973). Under the given conditions, one unit of activity corresponds to one micromole of NAD+ reduced each minute at 30 °C and pH 8.0. The reaction mixture includes 2.28 mL of 0.05 M Tris-HCl buffer (pH 8.0), 0.50 mL of 13.3 mM MgCl, 0.10 mL of 0.67 M Glucose above Tris-MgCl2, 0.10 mL of 16.5 mM ATP, 0.10 mL of 6.8 mM NAD, and 300 IU/mL of glucose-6-phosphate dehydrogenase. Increase in absorbance was taken for 3 mins.

The method published by Jagannathan et al. (1956) based on Boyer's adaptation of the hydrazine test, in which 3-phosphoglyceraldehyde interacts with hydrazine to create a hydrazone that absorbs at 240 nm, was used to determine the activity of aldolase (ALD).. The reaction mixture included 1.0 mL 0.012 M Fructose-1,6-bisphosphate (pH 7.5), 2.0 mL 0.0035 M Hydrazine sulfate in 0.0001 M EDTA (pH 7.5), 1.0 mL distilled water, 0.1 mL lung homogenate. Absorbance was taken for 3 min at 1min interval.

Lactate dehydrogenase activity (LDH) was determined using the manufacturer's protocol. The method described by Kim et al. (1993) was used to measure NADase activity. Cyanide reacts with the quaternary nitrogen form of NAD+ to produce an addition product with a maximum absorbance at 340 nm. As a result, the interaction between cyanide and NAD before and after being incubated with NADase shows that the enzyme is active. One unit of enzyme activity is that cleaving one micromole of NAD per minute at 37°C and pH 7.5. The reaction mixture consists of 0.3 mL 0.1 M potassium phosphate buffer pH 7.5, 0.1 mL 5.4 mM NAD, 3.0 mL 1.0M KCN. The above mixture was incubated at 37°C for 3-5 min to achieve temperature equilibration, allowed to cool and 0.1 mL lung homogenate added. Absorbance was taken for 3 min at 1min interval.

Determination of pulmonary tricarboxylic acid cycle enzymes activities in asthmatic mice

Citrate synthase (CS) catalyses the reaction of two-carbon acetyl CoA with four-carbon oxaloacetate to form six-carbon citrate, Coenzyme A is produced when citrate synthase (CS) catalyses the reaction of two-carbon acetyl CoA with four-carbon oxaloacetate to produce six-carbon citrate. The spectrophotometric enzyme test approach described by Yu et al. (2007) was used to measure the CS activity. Citrate synthase activity was evaluated by measuring the reaction product thionitrobenzoic acid (TNB) of 5,5′-dithiobis-(2-nitrobenzoic acid (DTNB) and coenzyme A (CoASH) at 412 nm.thus regenerating coenzyme A. The CS activity was assessed using the

spectrophotometric enzyme test methodology reported by Yu et al. (2007). By detecting the reaction product thionitrobenzoic acid (TNB) of 5,5′-dithiobis-(2-nitrobenzoic acid (DTNB) and coenzyme A (CoASH) at 412 nm, citrate synthase activity was determined. The rate of absorbance rise is inversely related to enzyme activity.

As previously stated by (Romkina & Kiriukhin, 2017), the isocitrate dehydrogenase (IDH) activity was routinely assessed by observing the decrease of NAD + at 340 nm (2017). Using a Vis spectrophotometer to measure the absorbance at 340 nm, the rise in NAD(P)H concentration was identified Malate dehydrogenase (MDH) activity was assessed by measuring the change in absorbance at 340 nm brought on by NADH oxidation. Under the specified conditions, one unit oxidizes one micromole of NADH per minute at 25 °C and pH 7.4. (Thorne, 1962). Thus, the following solution was pipetted into the cuvette; 2.6 mL 0.1 M Phosphate buffer, 0.2 mL NADH, 0.1 mL oxaloacetate, 0.1 mL of sample was added to the cuvette and change in absorbance for 3 min was followed at 30sec interval.

The activity of succinate dehydrogenase (SDH) was measured spectrophotometrically, according to the procedure described by Veeger et al. (1969). The following were added to a cuvette for a spectrophotometer analysis: 1 mL of pH 7.6 phosphate buffer, 30 mM EDTA, 0.3 mL of 0.4 m succinate, 0.1 m 3% BSA, and 0.2 m 75 mM K3FE(CN)6 are also required. The reaction was initiated at absorbance 455 nm by the addition of 25 µL of lung homogenate, and changes in absorbance were measured every 30 seconds for three minutes.

Determination of electron transport chain enzymes activities in asthmatic mice

According to Medja et al. (2009), Complex I activity (NADH ubiquinone oxidoreductase) was assessed in isolated mitochondria by measuring the oxidation of 100 M NADH in the presence and absence of 25 M rotenone at 340 nm. Using a technique developed by Medja et al. (2009), the activity of complex II (succinate ubiquinone oxidoreductase) was assessed spectrophotometrically at 600 nm. Complex III (cytochrome c oxidoreductase) activity was measured spectrophotometrically at 550 nm using the Medja et al. (2009) method. Respiratory complex III activity is calculated after evaluating the activity of ubiquinol cytochrome c oxidoreductase in the presence and absence of antimycin. From reduced cytochrome C, electrons are transferred to oxygen by respiratory chain complex IV. By monitoring the decline in cytochrome C absorbance at 550 nm, its activity was determined. 12 µL of 100 µM cytochrome C in 50 mM potassium phosphate buffer with a pH of 7.0 were put in a 15 mL test tube. 280 µL of buffered cytochrome c was added after 6 µL was pipetted into the cuvette. 3 minutes of absorbance measurements were conducted at 30-second intervals at 550nm.

Estimation of pulmonary levels of oncogenic and apoptotic (caspase-3, p53, Bax, Bcl-2, c-Myc, and Ras) factors in asthmatic mice

The ELISA kit instructions from Cusabio Technology Llc, Houston, TX, USA, were adhered to. In brief, wells treated with an antibody specific for caspase-3, p53, Bax, Bcl-2, c-Myc, or Ras were added 100 L of samples and standards (catalog no: Caspase 3- CSB-EL004543RA; p53- CSB-E08336r; Bax- CSB-EL002573RA; BCl-2- CSB-RA564360A0HU; c-Myc- CSB-PA02589A0Rb; Ras- CSB-PA13969A0Rb). The wells were then incubated for two hours at 37 C. After removing any unbound materials, 100 µL of biotin-conjugated antibody that was directed against caspase-3, p53, Bax, Bcl-2, c-Myc, or Ras was added to the well. Following washing, the wells were treated with 100 µL of avidin-conjugated Horseradish Peroxidase (HRP) and incubated for 1 hour at 37 C. Next, 90 µL of TMB substrate solution was added, and the wells were incubated for 15 to 30 minutes at 37 C to produce a colour proportional to the amount of caspase-3, p53, Bax, Bcl-2, c-Myc, or Ras bound in the initial step. The plate was lightly tapped for full mixing after adding stop solution to each well, and the color intensity was evaluated at 450 nm.

Histopathological analysis

Lung tissues were paraffin embedded, sectioned into 5 µm sections, deparaffinized, and stained with hematoxylin and eosin. Following Fisher et al. (2008) instructions. The microanatomy of lung tissue was examined under a light microscope (Nikon Diaphot, USA) (2008) (400 magnification). A pathologist performed the histopathological investigation and explanations.

Scoring of histopathological aberrations

Hematoxylin and eosin (H & E) staining was followed by histological scoring, which is depicted in Figure 9. The following rating criteria were employed in a semi-quantitative morphometric analysis scoring system to evaluate the lung injury. Normal appearance is represented by the number 0, mild interstitial hyperemia, polymorphonuclear leukocyte infiltration is represented by the number 1, paravascular edoema is represented by the number 2, moderate pulmonary structural damage is represented by the number 3, and severe lung structural damage is represented by the number 4. (Oishi et al., 2012). The histology examinations were all carried out under blind conditions. A pathologist quantitatively quantified the histology, and the scoring is shown in the

table below.

Table 1

Scoring of histopathological aberrations

Features observed	Scoring
Normal appearance	0
Mild interstitial hyperemia, polymorphonuclear leukocyte infiltration	1
Paravascular edoema	2
Moderate pulmonary structural damage	3
Severe lung structural damage	4

DiNP-induced aberrations in histological scoring

When compared to the control group (0.42), the considered parameters used to assess lung injury (i.e., Normal appearance; 1: Mild interstitial hyperemia, polymorphonuclear leukocyte infiltration; 2: Paravascular edoema and moderate pulmonary structural damage; 3: Massive cell infiltration and moderate alveolar structure destruction; and 4: Massive cell infiltration and severe lung structural damage) were significantly higher ($P<0.05$) in the DiNP-treated group (4.0+ 0.0) when compared with the control (0.42 ± 0.20).

Statistical analysis

The results were given as mean ±S.D. Data were analysed using the Tukey post hoc test and an ANOVA using Graphpad Prism (V 8.01). P values of 0.05 or below were regarded as statistically significant.

RESULTS

DiNP alters pulmonary oxidant-antioxidant system in asthmatic mice

Figure 3 depicts DiNP-induced alterations in the activities of enzymatic (CAT, SOD and GST) and concentrations of non-enzymatic (GSH and AA) antioxidants. When compared to control mice, exposure to DiNP caused a substantial decline in CAT (50%), GST (57%) SOD (70%) activities, and GSH (54%) and AA (76%) concentrations, as well as a concurrent rise in MDA (97%) levels ($p <0.05$).

DiNP-induces inflammation in asthmatic mice

Figure 4 depicts the changes in NO level and MPO activity brought on by DiNP. In the mice treated with DiNP alone, there was an increase in NO (80%) and MPO (49%), compared to the control mice ($p<0.05$).

DiNP alters glycolytic enzymes activities in asthmatic mice

The effect of DiNP on glycolytic enzymes activities is shown in Figure 5. Contrasted with the control group, DiNP downregulated the activities of HK (64%), ALD (58%), LDH (82%) and upregulated the activity of NADase (77%) ($p<0.05$).

DiNP alters tricarboxylic acid cycle enzymes activities in asthmatic mice

DiNP-induced alterations in tricarboxylic acid cycle enzymes activities is given in Figure 6. DiNP caused a significant decrease ($p<0.05$) in CS (72%), IDH (71%), MDH (64%) and SDH (77%) activities relative to the control group.

DiNP alters electron transport chain enzymes activities in asthmatic mice

Figure 7 shows DiNP-induced alterations in the activities of the electron transport chain enzymes. When compared to the control group, DiNP caused a significant decrease ($p<0.05$) in CMP I (55%), CMP II (87%), CMP III (88%) and CMP IV (85%) activities.

Figure 3

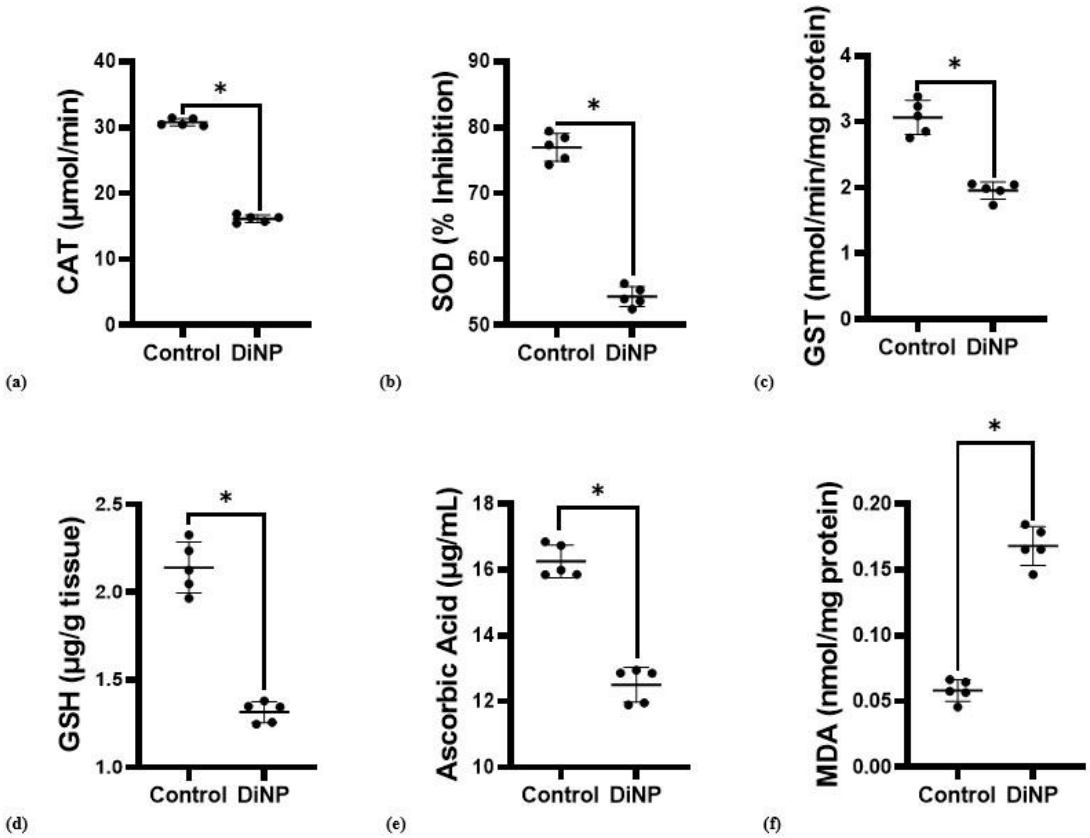

*Note: Pulmonary antioxidants (a) Catalase (CAT); (b) Superoxide dismutase (SOD); (c) Glutathione-S-transferase (CST) activities; Reduced glutathione (GSH); Ascorbic Acid levels; and oxidative stress biomarker (f) malondialdehyde (MDA) level. The values are expressed as Mean ± SD of 5 mice (n = 5) in each group. *DiNP significantly different from control (p < 0.05).*

Figure 4

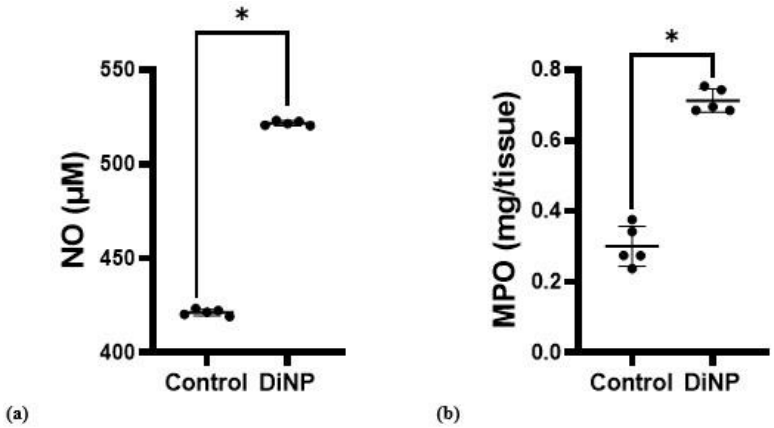

*Note: Pulmonary inflammatory (a) Nitric oxide (NO) level; and (b) Myeloperoxidase (MPO) activity. The values are expressed as Mean ± SD of 5 mice (n = 5) in each group. *DiNP significantly different from control (p < 0.05).*

Figure 5

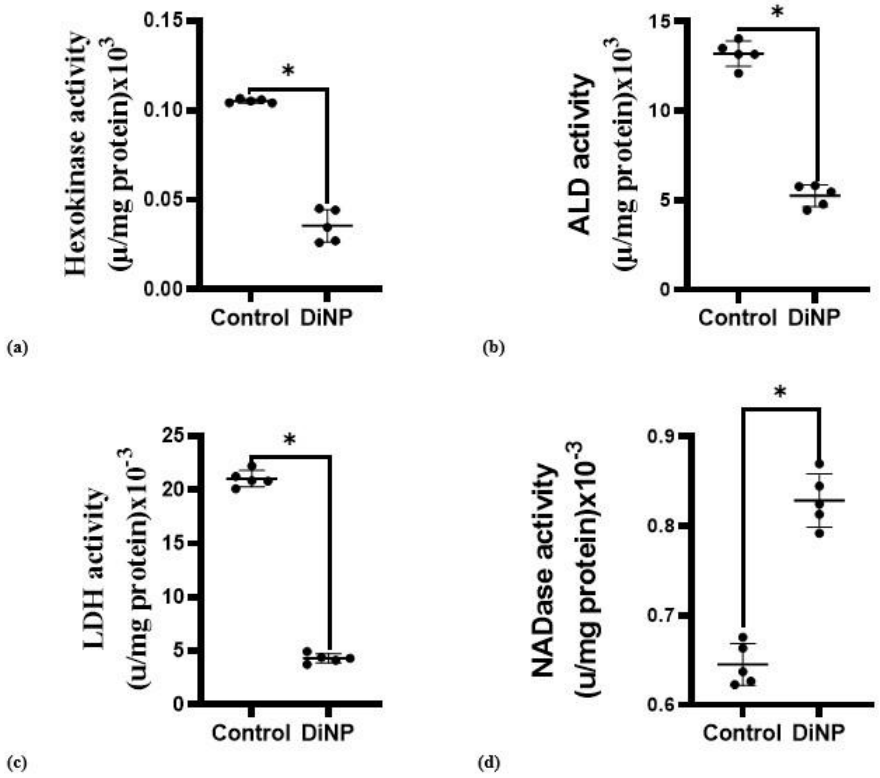

*Note: Pulmonary glycolytic (a) hexokinase (HK); (b) aldolase (ALD); (c) lactate dehydrogenase (LDH);(d) NADase (NAD glycohydrolase) enzyme activity. The values are expressed as Mean ± SD of 5 mice (n = 5) in each group. *DiNP significantly different from control (p < 0.05).*

Figure 6

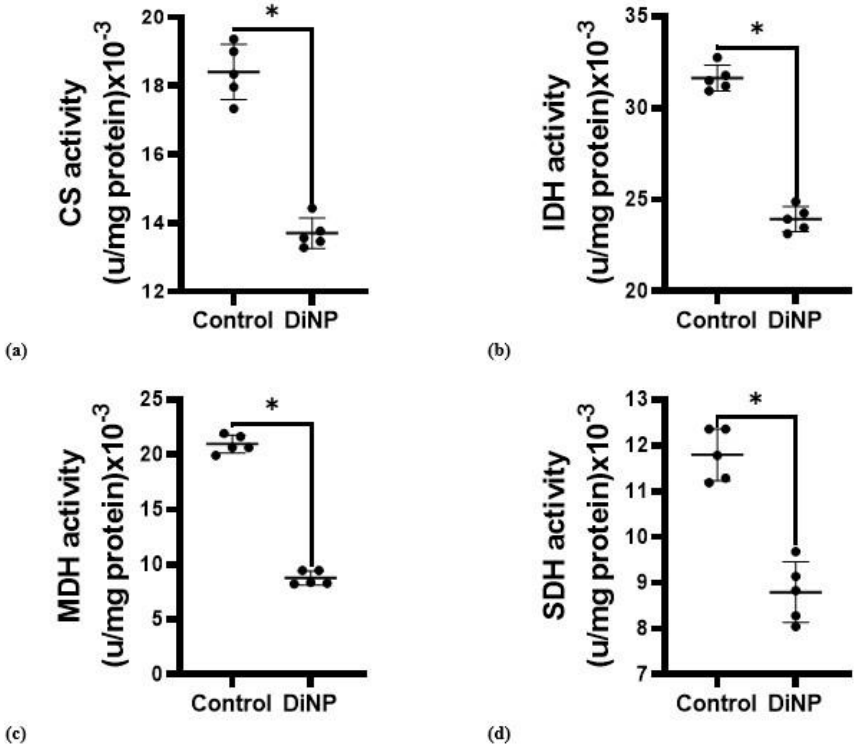

*Note: Pulmonary tricarboxylic acid cycle (a) citrate synthase (CS); (b) isocitrate dehydrogenase (IDH); (c) malate dehydrogenase (MDH);(d) succinate dehydrogenase (SDH) enzyme activity. The values are expressed as Mean ± SD of 5 mice (n = 5) in each group. *DiNP significantly different from control (p < 0.05).*

Figure 7

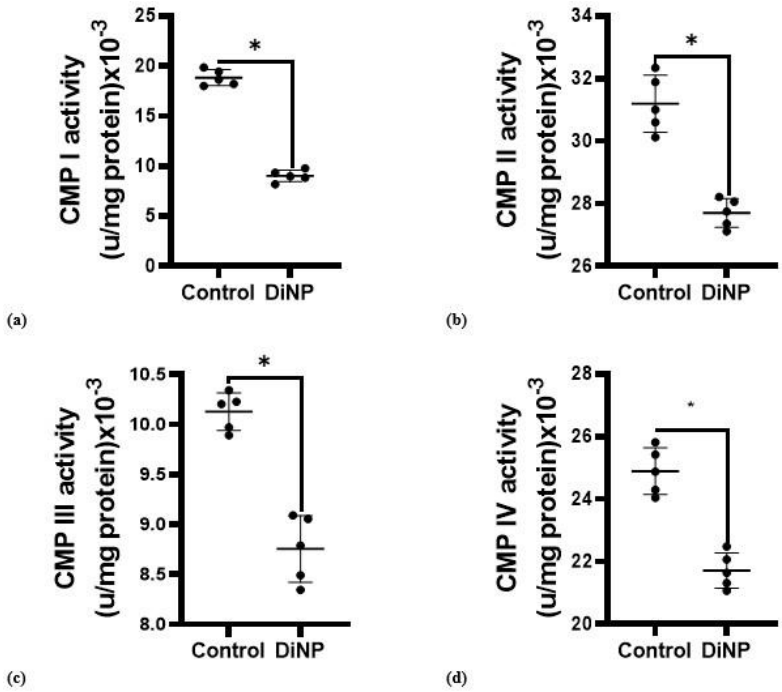

*Note: Pulmonary electron transport chain (a) complex I (CMP I); (b) complex II (CMP II); (c) complex III (CMP III) ;(d) complex IV (CMP IV) enzyme activity. The values are expressed as Mean ± SD of 5 mice (n = 5) in each group. *DiNP significantly different from control (p < 0.05).*

DiNP alters oncogenic and apoptotic factors levels in asthmatic mice

DiNP-induced changes in oncogenic and apoptotic factors levels is given in Figure 8. DiNP caused a significant decrease (p<0.05) in BCL-2 (74%), and increase in CAS-3 (65%), p53 (51%), Bax (70%), K-Ras (82%) and c-MYC (59%) activities relative to the control group.

Figure 8

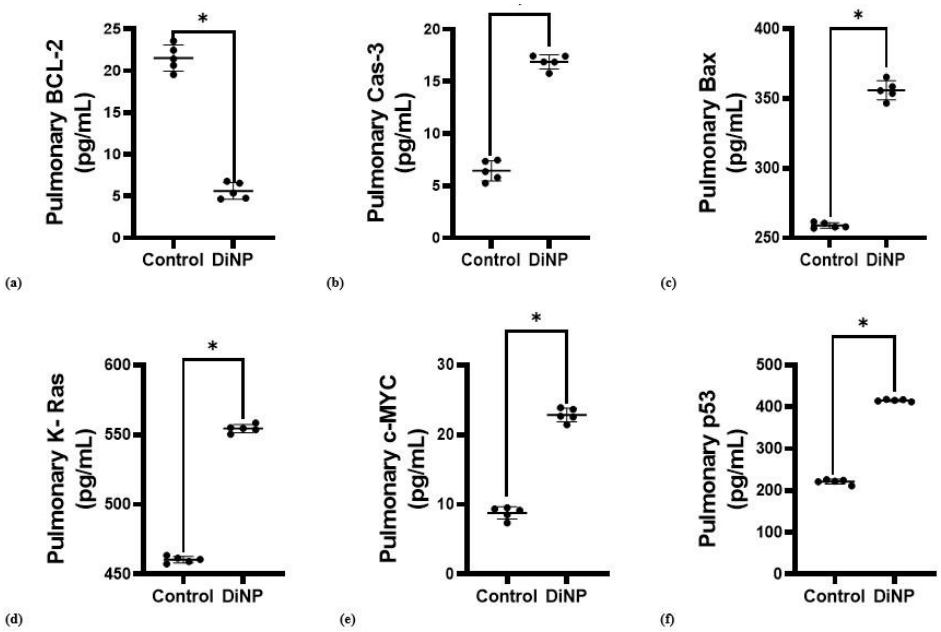

*Note: Pulmonary oncogenic and apoptotic (a) B-cell lymphoma 2 (BCL-2); (b) Caspase-3 (Cas-3); (c) Bax (Apoptosis regulator BAX); (d) K-Ras (Kirsten rat sarcoma virus); (e) c-MYC (Cellular Myelocytomatosis); (f) Tumor protein P53 (p53) factors. The values are expressed as Mean ± SD of 5 mice (n = 5) in each group. *DiNP significantly different from control (p < 0.05).*

DiNP alters the histoarchitecture of the lungs

Figure 9 showing how DiNP affects the histoarchitecture of the lung. Control mice in plate 1 displayed intact respiratory epithelial morphology, including the terminal bronchiole that leads into the alveoli duct. DiNP-treated animals, on the other hand, displayed a variety of pathologies, including deformed parenchyma, increased alveolar thickness, lymphocyte and neutrophil infiltration, fibrin deposition, pulmonary emphysema, pneumonia, intra alveolar haemorrhage, and oedema.

Figure 9

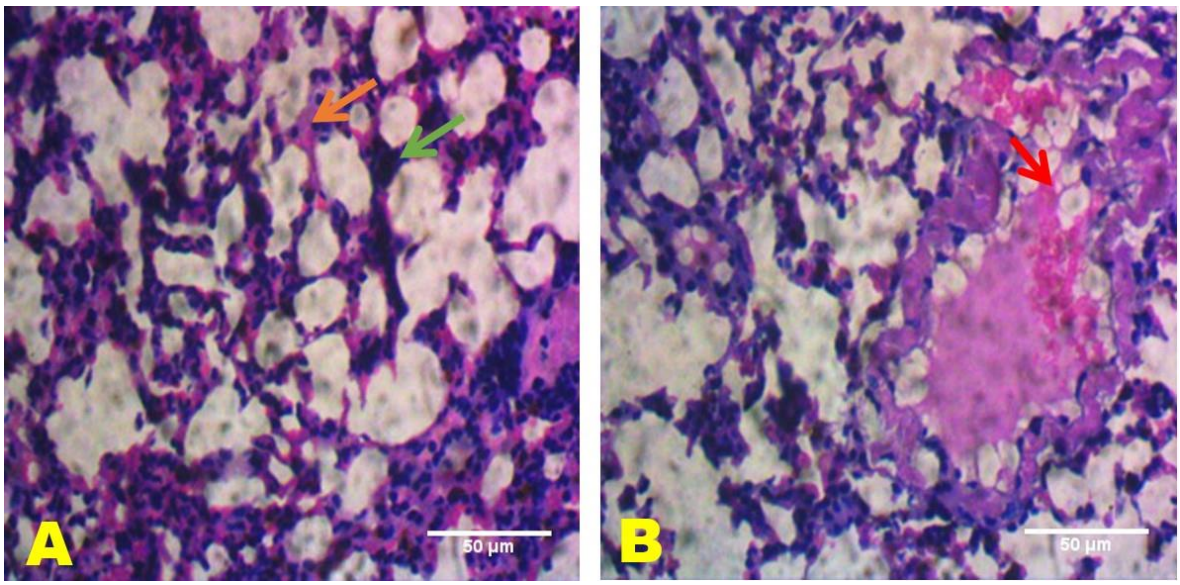

Note: Representative photomicrographs of Lung sections subjected to Hematoxylin and Eosin (H&E) stain (x400). A Control, B- DiNP. Orange arrow- smooth muscle, red arrow – severe oedema, congestion and distorted respiratory epithelium, Green arrow- megakaryocyte, Scale bar- 50µm.

DiNP-induced aberrations in histological scoring

When compared to the control group (0.42), the considered parameters used to assess lung injury (i.e., Normal appearance; 1: Mild interstitial hyperemia, polymorphonuclear leukocyte infiltration; 2: Paravascular edoema and moderate pulmonary structural damage; 3: Massive cell infiltration and moderate alveolar structure destruction; and 4: Massive cell infiltration and severe lung structural damage) were significantly higher ($P<0.05$) in the DiNP treated group (4.0+ 0.0) when compared with the control (0.42 ± 0.20; Fig. 10).

Figure 10

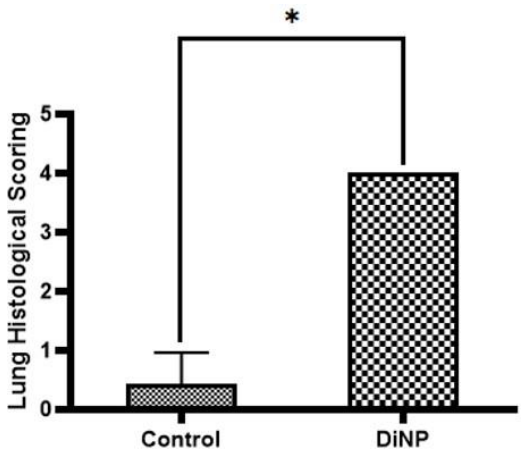

*Note: Histological scoring of lungs pathology following hematoxylin and eosin (H and E) staining. Values are expressed as mean ± SD, *- significantly different from control (P < 0.05).*

DISCUSSION

Asthma-related oxidative stress is receiving more and more attention in the scientific community. Inflammation of the airways is a hallmark of asthma. Inflammation has the potential to cause, contribute to, and/or result in oxidative stress. Reactive oxygen species (ROS) and other oxidative stressors are produced because of exposure to allergens and irritants such phthalates and a variety of other pollutants, which leads to an imbalance of antioxidants and oxidants. While some studies reveal elevated antioxidative activity in asthmatics, others find that asthmatics have a diminished ability to respond to oxidative stress. The Th(1)/Th(2) immune response may change as a result of oxidative stress, which can also activate NF-kbeta, a potent inducer of pro-inflammatory genes (Dozor, 2010). ROS are produced rapidly after the onset of asthma in both humans and laboratory animals. ROS influence the structure and functionality of the airways (Sahiner et al., 2018). From this study, the experimental group that received DiNP had a significant decreased in the activities of enzymatic antioxidants (CAT, SOD, GST) and decreased concentration of non-enzymatic antioxidants (GSH, AA). An imbalance between the antioxidant-oxidant localised in the lungs of DiNP-treated animals or an excessive production of ROS are responsible for this reduction. The oxidative destruction of lipids is referred to as lipid peroxidation. Many biochemical techniques have used MDA, a by-product of lipid peroxidation, to gauge the extent of oxidative damage in asthma (Tang et al., 2021). The findings of this study show that DiNP significantly increased level of MDA. An elevated amount of MDA in the lung of the DiNP-treated group indicates a higher degree of lipid peroxidation and a depletion of antioxidants, which causes lung membrane to be exposed to lipid oxidation. As mentioned earlier, oxidative stress may activate NF-kbeta, a potent inducer of pro-inflammatory genes. This is evident in the findings of this research as DiNP upregulated NO levels and MPO activity, both which are markers of inflammation. The results of this study concur with those of Olajide et al. (2023). MPO, a protein found in high concentrations in neutrophils, monocytes, and certain subpopulations of tissue macrophages, is thought to be crucial for both host defences and inflammatory tissue injury. The heme core of the enzyme may catalyse oxidation reactions that result in the creation of a range of diffusible radicals and reactive oxidant species to carry out these functions. The primary granules of active leukocytes are where MPO and inducible nitric-oxide synthase (iNOS), which both play crucial roles in inflammation, are stored, and released (Abu-Soud & Hazen, 2000).

Chemical energy is required for most cell activity. The cellular process of releasing energy from food and storing it as ATP is known as respiration. Fundamental to both respiratory and non-respiratory function is lung cellular metabolism. The lung depends heavily on circulating substrates and has a relatively small energy store. The pattern of substrate use is significantly influenced by the availability of substrates, competition between different substrates, and the uptake and metabolic capability of lung cells. The lung uses a range of substrates as essential building blocks for synthesis, energy-producing fuels, sources of NADPH for lipid biosynthesis, and sources of glutathione. These substrates include glucose, lactate, fatty acids, choline, ketone bodies, and amino acids (Liu & Summer, 2019). Despite being a metabolically busy organ that's occasionally overlooked, biochemical studies have long shown that the lung uses glucose more efficiently than many other organs, including the heart, kidney, and brain. The beating of cilia or the generation of surfactant are two examples of highly specialized energy-consuming actions carried out by specific lung cell populations (Liu & Summer, 2019). According to da Cunha et al. (2014) lung injury influences how the body uses its energy. In their investigation, rats subjected to lung damage showed decreased activities of the electron transport chain's enzymes succinate dehydrogenase, complex II, cytochrome c oxidase, and ATP levels, as well as the emergence of pulmonary oedema. The findings of this investigation are consistent with those of da Cunha et al. (2014); considerable downregulation of the glycolytic (HK, ALD, LDH), TCA (CS, IDH, MDH, SDH), and electron transport chain (CMP I, II, III, IV) enzymes was discovered. Our results suggest that mitochondrial dysfunction may be one of the primary causes of lung damage.

Apoptosis is a crucial stage of planned cell death that is present in both healthy and malignant tissues. Apoptosis causes damaged or mutated cells to die in healthy tissues, stopping future mutations and the development of cancer. Many clinical disorders, including malignancies, may be brought on by modifications to the nature of apoptosis (Thompson, 1995). For apoptosis and cell cycle arrest in DNA damage and cell injury, P53 is a key tumour suppressor protein (Aubrey et al., 2018). When there is no cellular damage, it manifests in the cytosol at low levels and is predominantly regulated by the murine double minute oncogene (MDM2) (Momand et al., 2000). P53 begins to build up in the nucleus because of DNA damage brought on by UV radiation or other environmental causes. It causes cell cycle arrest and death, which stop future mutations and the development of cancer (Chen, 2016). Apoptosis can be either promoted or inhibited by the Bcl-2 protein family (Erb et al., 2005). By interacting with pro-apoptotic proteins and inhibiting apoptosis, it promotes cell survival. Most malignancies with high levels of Bcl-2 expression have poor prognoses, and alterations to Bcl-2 protein levels are a key mechanism for carcinogenesis (Czabotar et al., 2014). Proapoptotic protease family member caspase-3 causes nuclear modifications that cause apoptosis (Boland et al., 2013). In addition to being enhanced as a favourable prognostic indicator for gastric malignancies, caspase-3 levels are decreased in numerous cancer types, including cervical and breast cancer (Xu et al., 2013; Huang et al., 2018). Through weakening mitochondrial integrity, c-Myc encourages apoptosis and causes the release of proapoptotic effectors such holocytochrome c. The members of the Bcl-2 family that promote apoptosis are potential mediators of c-Myc in this process (Bai et al., 2023). Bax, a controller of apoptosis, regulates either pro- or anti-apoptotic activities in a variety of cellular processes. The voltage-dependent anion channel (VDAC) in the mitochondria is said to interact with Bax and be encouraged to

open, which causes a decrease in membrane potential and the release of cytochrome c. This gene's expression has been linked to P53-mediated apoptosis and is controlled by the tumour suppressor P53. Bax activation has been demonstrated to be in association with overexpression of c-MYC (Annis et al., 2005). By transmitting mitogenic and growth signals into the cytoplasm and nucleolus, K-Ras participates in a variety of ligand-mediated signal transduction pathways and affects proliferation, differentiation, transformation, and death (Papke & Der, 2017).

From this study, all apoptotic factors were significantly increased in DiNP-treated group, however, Bcl-2 level decreased in DiNP-treated group in comparison to control. It is important to highlight that bcl-2 overexpression in some cancer cells may suppress the pro-apoptotic signals that allow cancer cells to survive in stressful situations, whereas bcl-2 at low levels may have the opposite effect. Although Bcl-2 helps malignant cells survive and increases their ability to fight drugs, but it also presents chances for cutting-edge targeted therapies that kill such cells only (Hafezi & Rahmani, 2021). Hence, studying Bcl-2 in DiNP-induced lung cancer may provide therapies for its treatment.

The airways of asthmatic patients constrict when they are exposed to allergens or asthma triggers. Mucus is overexpressed, irritated, and tightened due to enlarged walls and inflammation in contrast to the airways of healthy people which possess a normal airway wall, and relaxed smooth muscle (Shastri et al., 2021). DiNP caused airway inflammation histologically by infiltrating inflammatory cells, oedema, haemorrhage, and limited alveoli space in this study and this is consistent with those of Olajide et al. (2023).

CONCLUSION

This study examined mitochondrial oxidative stress, inflammation, changes in energy metabolising enzymes, apoptotic factors, and histoarchitecture in the lungs of a mouse model of DiNP-induced asthma. This study suggests that DiNP negatively affects pulmonary antioxidant status, which activates inflammatory markers, inhibits energy metabolism by inhibiting energy transduction enzymes, which results in inhibition of the synthesis and breakdown of ATP, suggesting that the lungs don't produce enough ATP to carry out their respiratory and non-respiratory functions, and promotes the actions of apoptotic factors that may induce cancer.

AUTHOR CONTRIBUTIONS

The study's concept, design, and research materials were all produced by Samuel Abiodun Kehinde. The study's laboratory analysis, data collection and organization were handled by Abosede Temitope Olajide and Akinpelu Oyindamola Joy. The data were analysed and evaluated by Abosede Temitope Olajide and Akinpelu Oyindamola Joy. The article's first and last draft were written by Samuel Abiodun Kehinde and Abosede Temitope Olajide. Histopathological analysis and interpretation and review of the first draft were done by Sanmi Tunde Ogunsaya.

ETHICS APPROVAL

The Ethical Review Committee of the Faculty of Natural Sciences at Ajayi Crowther University gave its approval to the study's experimental design FNS/ERC/23/005AP.

FUNDING

No specific grant was given to this research by funding organisations in the public, private, or not-for-profit sectors.

CONFLICTS OF INTEREST

The authors declare no conflict of interest in this work.

ACKNOWLEDGEMENTS

The authors are thankful to the Biochemistry unit of the Department of Chemical Sciences, Ajayi Crowther University, Oyo and Mr. Raphael Kolade for the provision of reagents, laboratory and other facilities.

REFERENCES

Abu-Soud, H. M., & Hazen, S. L. (2000). Nitric oxide modulates the catalytic activity of myeloperoxidase. *Journal of Biological Chemistry*, *275*(8), 5425-5430. https://doi.org/10.1074/jbc.275.8.5425

Annis, M. G., Soucie, E. L., Dlugosz, P. J., Cruz-Aguado, J. A., Penn, L. Z., Leber, B., & Andrews, D. W. (2005). Bax forms multispanning monomers that oligomerize to permeabilize membranes during apoptosis. *The EMBO Journal*, *24*(12), 2096-2103. https://doi.org/10.1038/sj.emboj.7600675

Aubrey, B. J., Kelly, G. L., Janic, A., Herold, M. J., & Strasser, A. (2018). How does p53 induce apoptosis and how does this relate to p53-mediated tumour suppression?. *Cell Death & Differentiation*, *25*(1), 104-113. https://doi.org/10.1038/cdd.2017.169

Bai, L., Zhou, L., Han, W., Chen, J., Gu, X., Hu, Z., ... & Cui, J. (2023). BAX as the mediator of C-MYC sensitizes acute lymphoblastic leukemia to TLR9 agonists. *Journal of Translational Medicine*, *21*(1), 1-18. https://doi.org/10.1186/s12967-023-03969-z

Boland, K., Flanagan, L., & Prehn, J. H. (2013). Paracrine control of tissue regeneration and cell proliferation by Caspase-3. *Cell Death & Disease*, *4*(7), e725-e725. https://doi.org/10.1038/cddis.2013.250

Buege, J. A., & Aust, S. D. (1978). [30] Microsomal lipid peroxidation. In *Methods in Enzymology* (Vol. 52, pp. 302-310). Academic Press. https://doi.org/10.1016/S0076-6879(78)52032-6

Chen, J. (2016). The cell-cycle arrest and apoptotic functions of p53 in tumor initiation and progression. *Cold Spring Harbor Perspectives in Medicine*, *6*(3), a026104. https://doi.org/10.1101/cshperspect.a026104

Colowick, S.P. (1973). The Hexokinases, in: The Enzymes, 9, Academic Press, 1973, pp. 1– 48. https://doi.org/10.1016/S1874-6047(08)60113-4

Czabotar, P. E., Lessene, G., Strasser, A., & Adams, J. M. (2014). Control of apoptosis by the BCL-2 protein family: implications for physiology and therapy. *Nature Reviews Molecular Cell Biology*, *15*(1), 49-63. https://doi.org/10.1038/nrm3722

Da Cunha, M. J., Da Cunha, A. A., Scherer, E. B., Machado, F. R., Loureiro, S. O., Jaenisch, R. B., ... & Wyse, A. T. (2014). Experimental lung injury promotes alterations in energy metabolism and respiratory mechanics in the lungs of rats: prevention by exercise. *Molecular and Cellular Biochemistry*, *389*, 229-238. https://doi.org/10.1007/s11010-013-1944-8

Dozor, A. J. (2010). The role of oxidative stress in the pathogenesis and treatment of asthma. *Ann N Y Acad Sci,* 1203:133-137. https://doi.org/10.1111/j.1749-6632.2010.05562.x

Erb, P., Ji, J., Wernli, M., Kump, E., Glaser, A., & Büchner, S. A. (2005). Role of apoptosis in basal cell and squamous cell carcinoma formation. *Immunology Letters*, *100*(1), 68-72. https://doi.org/10.1016/j.imlet.2005.06.008

Fischer, A. H., Jacobson, K.A., Rose, J., & Zeller, R. (2008). Cold Spring Harbor Protocols 5 4986 pdb.prot. https://doi.org/10.1101/pdb.prot073411

Green, L. C., Wagner, D. A., Glogowski, J., Skipper, P. L., Wishnok, J. S., & Tannenbaum, S. R. (1982). Analysis of nitrate, nitrite, and [15N] nitrate in biological fluids. *Analytical Biochemistry*, *126*(1), 131-138. https://doi.org/10.1016/0003-2697(82)90118-X

Habig, W. H., Pabst, M. J., & Jakoby, W. B. (1974). Glutathione S-transferases: the first enzymatic step in mercapturic acid formation. *Journal of Biological Chemistry*, *249*(22), 7130-7139. https://doi.org/10.1016/S0021-9258(19)42083-8

Hafezi, S., & Rahmani, M. (2021). Targeting BCL-2 in cancer: advances, challenges, and perspectives. *Cancers*, *13*(6), 1292. https://doi.org/10.3390/cancers13061292

Hsieh, T. H., Tsai, C. F., Hsu, C. Y., Kuo, P. L., Lee, J. N., Chai, C. Y., ... & Tsai, E. M. (2012). Phthalates induce proliferation and invasiveness of estrogen receptor-negative breast cancer through the AhR/HDAC6/c-Myc signaling pathway. *The FASEB Journal*, *26*(2), 778-787. https://doi.org/10.1096/fj.11-191742

Huang, K. H., Fang, W. L., Li, A. F. Y., Liang, P. H., Wu, C. W., Shyr, Y. M., & Yang, M. H. (2018). Caspase-3, a key apoptotic protein, as a prognostic marker in gastric cancer after curative surgery. *International Journal of Surgery*, *52*, 258-263. https://doi.org/10.1016/j.ijsu.2018.02.055

Hwang, Y. H., Paik, M. J., & Yee, S. T. (2017). Diisononyl phthalate induces asthma via modulation of Th1/Th2 equilibrium. *Toxicology Letters*, *272*, 49-59. https://doi.org/10.1016/j.toxlet.2017.03.014

Jagannathan, V., Singh, K., & Damodaran, M. (1956). Carbohydrate metabolism in citric acid fermentation. 4. Purification and properties of aldolase from Aspergillus niger. *Biochemical Journal*, *63*(1), 94. https://doi.org/10.1042/bj0630094

Jagota, S. K., & Dani, H. M. (1982). A new colorimetric technique for the estimation of vitamin C using Folin phenol reagent. *Analytical Biochemistry*, *127*(1), 178-182. https://doi.org/10.1016/0003-2697(82)90162-2

Kehinde, S. A., Olajide A. T., Ore, A., & Ogunsanya, S. T. (2023). Disruption of Renal Energy Metabolism Dynamics and Histoarchitecture in Diisononyl Phthalate-Exposed Wistar Rats. Biomed J Sci & Tech Res 48(4)-2023. BJSTR. MS.ID.007679. https://doi.org/10.26717/BJSTR.2023.48.007679

Kehinde, S. A., Ore, A., Olajide, A. T., Ajagunna, I. E., Oloyede, F. A., Faniyi, T. O., & Fatoki, J. O. (2022a). Diisononyl phthalate inhibits cardiac glycolysis and oxidative phosphorylation by down-regulating cytosolic and mitochondrial energy metabolizing enzymes in murine model. *Advances in Redox Research*, *6*, 100041. https://doi.org/10.1016/j.arres.2022.100041

Kehinde, S., Ore, A., Olayinka, E., & Olajide, A. (2022b). Inhibition of hepatic energy metabolizing enzymes in murine model exposed to diisononyl phthalate. *Baghdad Journal of Biochemistry and Applied Biological Sciences*, *3*(04). https://doi.org/10.47419/bjbabs.v3i04.166

Kim, J. J., Shajib, M. S., Manocha, M. M., & Khan, W. I. (2012). Investigating intestinal inflammation in DSS-induced model of IBD. *Journal of Visualized Experiments: JoVE*, (60). https://doi.org/10.3791/3678

Kim, U. H., Han, M. K., Park, B. H., Kim, H. R., & An, N. H. (1993). Function of NAD glycohydrolase in ADP-ribose uptake from NAD by human erythrocytes. *Biochimica et Biophysica Acta (BBA)-Molecular Cell Research*, *1178*(2), 121-126. https://doi.org/10.1016/0167-4889(93)90001-6

Liao, P. C., Bergamini, C., Fato, R., Pon, L. A., and Pallotti, F. (2020). Isolation of mitochondria from cells and tissues. *Methods Cell Biol*., 155:3-31. https://doi.org/10.1016/bs.mcb.2019.10.002

Li, C. H. E. N., Jiao, C. H. E. N., Xie, C. M., Yan, Z. H. A. O., Xiu, W. A. N. G., & Zhang, Y. H. (2015). Maternal disononyl phthalate exposure activates allergic airway inflammation via stimulating the phosphoinositide 3-kinase/Akt pathway in rat pups. *Biomedical and Environmental Sciences*, *28*(3), 190-198.

Liu, G., & Summer, R. (2019). Cellular metabolism in lung health and disease. *Annual review of physiology*, *81*, 403-428. https://doi.org/10.1146/annurev-physiol-020518-114640

Medja, F., Allouche, S., Frachon, P., Jardel, C., Malgat, M., De Camaret, B. M., ... & Lombès, A. (2009). Development and implementation of standardized respiratory chain spectrophotometric assays for clinical diagnosis. *Mitochondrion*, *9*(5), 331-339. https://doi.org/10.1016/j.mito.2009.05.001

Misra, H. P., & Fridovich, I. (1972). The role of superoxide anion in the autoxidation of epinephrine and a simple assay for superoxide dismutase. *Journal of Biological Chemistry*, *247*(10), 3170-3175. https://doi.org/10.1016/S0021-9258(19)45228-9

Momand, J., Wu, H. H., & Dasgupta, G. (2000). MDM2—master regulator of the p53 tumor suppressor protein. *Gene*, *242*(1-2), 15-29. https://doi.org/10.1016/S0378-1119(99)00487-4

Moron, M. S., Depierre, J. W., & Mannervik, B. (1979). Levels of glutathione, glutathione reductase and glutathione S-transferase activities in rat lung and liver. *Biochimica et Biophysica Acta (BBA)-General Subjects*, *582*(1), 67-78. https://doi.org/10.1016/0304-4165(79)90289-7

Oishi, H., Takano, K., Tomita, K., Takebe, M., Yokoo, H., Yamazaki, M., & Hattori, Y. (2012). Olprinone and colforsin daropate alleviate septic lung inflammation and apoptosis through CREB-independent activation of the Akt pathway. *American Journal of Physiology Lung Cellular and Molecular Physiology*, 303(2), L130–L140. https://doi.org/10.1152/ajplung.00363.2011

Olajide, A.T., Olayinka, E.T**.,** Ore, A., Kehinde, S.A., & Okoye, C.C. (2023). Ellagic acid alleviates pulmonary inflammation and oxidative stress in mouse model of diisononyl phthalate-induced asthma. *Life Sciences, Medicine and Biomedicine*, *7*(1). https://doi.org/10.28916/lsmb.7.1.2023.110

Papke, B., & Der, C. J. (2017). Drugging RAS: Know the enemy. *Science*, *355*(6330), 1158-1163. https://doi.org/10.1126/science.aam7622

Pawankar, R. (2014). Allergic diseases and asthma: a global public health concern and a call to action. *World Allergy Organization Journal*, *7*(1), 1-3. https://doi.org/10.1186/1939-4551-7-12

Romkina, A. Y., & Kiriukhin, M. Y. (2017). Biochemical and molecular characterization of the isocitrate dehydrogenase with dual coenzyme specificity from the obligate methylotroph Methylobacillus Flagellatus. *Plos one*, *12*(4), e0176056. https://doi.org/10.1371/journal.pone.0176056

Sahiner, U. M., Birben, E., Erzurum, S., Sackesen, C., & Kalayci, Ö. (2018). Oxidative stress in asthma: Part of the puzzle. *Pediatric Allergy and Immunology*, 29(8), 789-800. https://doi.org/10.1111/pai.12965

Schmidt, J. J., & Colowick, S. P. (1973). Chemistry and subunit structure of yeast hexokinase isoenzymes. *Archives of Biochemistry and Biophysics*, *158*(2), 458-470. https://doi.org/10.1016/0003-9861(73)90537-7

Shastri, M. D., Chong, W. C., Dua, K., Peterson, G. M., Patel, R. P., Mahmood, M. Q., Tambuwala, M., Chellappan, D. K., Hansbro, N. G., Shukla, S. D., & Hansbro, P. M. (2021). Emerging concepts and directed therapeutics for the management of asthma: regulating the regulators. *Inflammopharmacology*, 29(1):15-33. https://doi.org/10.1007/s10787-020-00770-y

Sinha, A. K. (1972). Colorimetric assay of catalase. *Analytical biochemistry*, *47*(2), 389-394. https://doi.org/10.1016/0003-2697(72)90132-7

Tang, J., Yuan, Y., Wei, C., Liao, X., Yuan, J., Nanberg, E., ... & Yang, X. (2015). Neurobehavioral changes induced by di (2-ethylhexyl) phthalate and the protective effects of vitamin E in Kunming mice. *Toxicology Research*, *4*(4), 1006-1015. https://doi.org/10.1039/C4TX00250D

Tang, W., Dong, M., Teng, F., Cui, J., Zhu, X., Wang, W., ... & Wei, Y. (2021). Environmental allergens house dust mite-induced asthma is associated with ferroptosis in the lungs. *Experimental and Therapeutic Medicine*, 22(6), 1-10. https://doi.org/10.3892/etm.2021.10918

Thompson, C. B. (1995). Apoptosis in the pathogenesis and treatment of disease. *Science*, *267*(5203), 1456-1462. https://doi.org/10.1126/science.7878464

Thorne, C. J. R. (1962). Properties of mitochondrial malate dehydrogenases. *Biochimica et Biophysica Acta*, *59*(3), 624-633. https://doi.org/10.1016/0006-3002(62)90642-X

Veeger, C., DerVartanian, D. V., & Zeylemaker, W. P. (1969). [16] Succinate dehydrogenase: [EC 1.3. 99.1 Succinate:(acceptor) oxidoreductase]. In *Methods in Enzymology* (Vol. 13, pp. 81-90). Academic press. https://doi.org/10.1016/0076-6879(69)13020-7

Xu, M., Xia, L. P., Fan, L. J., Xue, J. L., Shao, W. W., & Xu, D. (2013). Livin and caspase-3 expression are negatively correlated in cervical squamous cell cancer. *European Journal of Gynaecological Oncology*, *34*(2), 152-155.

Yu, X., Tesiram, Y. A., Towner, R. A., Abbott, A., Patterson, E., Huang, S., ... & Kem, D. C. (2007). Early myocardial dysfunction in streptozotocin-induced diabetic mice: a study using in vivo magnetic resonance imaging (MRI). *Cardiovascular Diabetology*, *6*(1), 1-8. https://doi.org/10.1186/1475-2840-6-6

Citation:
Kehinde, S. A., Olajide, A. T., Akinpelu, O. J., & Ogunsanya , S. T.. (2023). Alteration of pulmonary mitochondrial oxidation status, inflammation, energy metabolizing enzymes, oncogenic and apoptotic markers in mice model of diisononyl phthalate-induced asthma. *Life Sciences, Medicine and Biomedicine*, *7*(1).
https://doi.org/10.28916/lsmb.7.1.2023.113

Life Sciences, Medicine and Biomedicine
ISSN: 2600-7207